The British Journal of Radiology, 85 (2012), 672–681

REVIEW ARTICLE

Review of the principal extra spinal pathologies causing sciatica and new MRI approaches

[1]A AILIANOU, MD, [4]A FITSIORI, MD, [1]A SYROGIANNOPOULOU, MD, [1]S TOSO, MD, [1]M VIALLON, PhD, [1]L MERLINI, MD, [2]J Y BEAULIEU, MD and [3]M I VARGAS, MD

[1]*Department of Radiology, Geneva University Hospital and University of Geneva, Geneva, Switzerland,* [2]*Hand Surgery Unit, Geneva University Hospital and University of Geneva, Geneva, Switzerland,* [3]*Department of Neuroradiology, Geneva University Hospital and University of Geneva, Geneva, Switzerland, and* [4]*Ioannina General Hospital, Ioannina, Greece*

ABSTRACT. In this paper we illustrate the principal extraspinal pathologies causing sciatica and new approaches for the study of structures such as the lumbosacral plexus (LSP). Visualisation of the LSP in its entirety is difficult with conventional two-dimensional MRI sequences owing to its oblique orientation. In our institution, we have found that the utilisation of three-dimensional short tau inversion-recovery sampling perfection with application-optimised contrasts using different flip angle evolutions sequence is helpful, allowing multiplanar and maximum intensity projection reconstructions in the coronal oblique plane and curvilinear reformats through the plexus. Diffusion tensor imaging enables the observation of microstructural changes and can be useful in surgical planning. The normal anatomy of the LSP, its different extraspinal pathologies and differential diagnoses are thoroughly presented.

Received 18 August 2010
Revised 21 June 2011
Accepted 4 July 2011

DOI: 10.1259/bjr/84443179

Sciatica, the pain resulting from irritation of the sciatic nerve, is a very common symptom, causing different levels of impairment, with increasing frequency in older populations, important economic consequences due to the loss of working hours and difficulty in its therapeutic approach. Most frequently a herniated disc at the level of the inferior lumbar spine is the cause; however, numerous extraspinal pathologies [1] can affect the lumbosacral plexus (LSP) and may be the origin of this symptom.

Spinal causes, including herniated nucleus pulposus, are probably the most common aetiologies of severe sciatica, and it is necessary to emphasise clinical differences between extraspinal LSP lesions and disc herniation. Symptoms vary greatly depending on the position and the size of the herniated disc.

Usually, sciatica begins suddenly, may be intermittent or constant and may worsen with increased intra-abdominal pressure, as in coughing. It may be relieved in the supine position, which decreases pressure on the herniated disc, and is aggravated by sitting, bending or prolonged standing. Stretching of the nerve reproduces pain in the sciatic distribution—the so-called Lasègue sign [2]. Numbness in one leg and muscular weakness may also occur.

Extraspinal radiculopathy can result in lower extremity pain, sensory disturbance and weakness. The pain pattern and accompanying symptoms are the major factors suggesting a non-discogenic aetiology of sciatica. In neoplastic plexopathies, the pain onset is usually insidious, prominent in one leg and is often the initial symptom of the disease.

Additional neurological symptoms such as weakness, gait dysfunction, sensory impairment, reflex impairment, paresthesias or dysesthesias are also frequent. Lower extremity oedema may also be encountered.

Our experience and a review of the current literature suggest that these extraspinal pathologies may be underestimated by radiologists and the referring physicians.

Recent advances in imaging, especially in MRI, with the evolution of older techniques, as well as the introduction of newer ones, such as diffusion tensor imaging (DTI), now enables a thorough exploration even of fine anatomic structures such as the LSP. For these reasons, we decided to present, in this paper, the commonest extraspinal pathologies causing sciatica after a brief presentation of the normal anatomy of the LSP, studied by conventional and new imaging techniques in our institution.

Imaging techniques: conventional and new approaches

The modality of choice for examining the sciatic nerve is MRI. However, CT can be useful, particularly in the setting of trauma or malignancy. The CT or MRI study protocol must be compatible with the pathology suspected. MRI studies are performed in the supine position with the combined use of the body and spinal coils. Our

Address correspondence to: Dr Maria Isabel Vargas, Department of Neuroradiology, DISIM, Geneva University Hospital, 4 Gabrielle-Perret-Gentil, 1211 Genève 14, Switzerland. E-mail: maria.i.vargas@hcuge.ch

standard imaging protocol comprises three-dimensional (3D) short tau inversion-recovery (STIR) sampling perfection with application-optimised contrast using different flip angle evolutions (SPACE) sequence, as well as T_1 and T_2 weighted imaging sequences in axial or coronal planes.

Conventional MRI that includes T_1 and T_2 weighted sequences provides anatomical and physiological information, thus helping to determine the location and characterisation of various LSP pathologies. T_1 and T_2 weighted images in the sagittal and axial planes are typically performed for evaluation of sciatica caused by abnormalities in the spinal canal. Peripheral nerves are isointense compared with muscle on the T_1 weighted images and generally appear slightly hyperintense on two-dimensional (2D) or 3D STIR and T_2 weighted sequences. T_1 axial images may be helpful, particularly in the case of extraforaminal disc herniation. Increased signal intensity may be seen on T_2 and STIR images, suggesting oedema or demyelination [3]; enhanced T_1 images can reveal abnormalities in functionally impaired nerves. Increased signal intensity, blurring and enlargement is often visualised in cases of nerve injury. However, increased neural signal intensity does not always indicate underlying disease. The magic angle effect is a well-recognised artefact in brachial plexus and lumbosacral plexus imaging. Chappell et al were the first to describe this phenomenon in peripheral nerve imaging [4]. The use of fat saturation sequences after intravenous administration of contrast agent is necessary when a tumoral, inflammatory or infectious pathology is suspected.

The 3D STIR SPACE sequence, which offers an excellent T_2-like contrast when long repetition times are used, is helpful to demonstrate the post-ganglionic [5, 6] nerve roots of the entire lumbosacral plexus with a sufficiently high resolution in a variety of pathological conditions. It is useful for the initial screening of patients with neoplastical conditions involving the LSP and it is a valuable tool for the depiction of nerve site compression. In our institution, each 3D STIR acquisition (echo time 1=149 ms, repetition time=2000 ms, inversion time=160 ms, turbo factor=73, time of acquisition=6–7 min, field of view=256, matrix size=256×260, number of slices $\geq$96, isotropic voxel size=0.9–1 mm^3) consists of a large coronal slab with approximately 96 partitions centred on the LSP with a right–left phase encoding direction. For each patient, multiplanar reconstruction (MPR) and thin maximum intensity projection (MIP) reconstructions are routinely obtained through the plexus in the coronal, coronal oblique and curvilinear planes. This is advantageous because complete coverage of the lumbosacral plexus is possible at a reasonable acquisition time. Comparison with the contralateral side is useful when a slight signal anomaly exists. The coronal oblique and curved reformatted imaging planes as well as the thin MIP allow for a reliable reconstruction of the nerve course from the spinal cord to the periphery and the simultaneous display of bone marrow contrast, which plays an important role in musculoskeletal pathologies.

DTI tractography [7–9] allows for 3D visualisation of neuronal fibres by using diffusion tensor data. Hence, by measuring diffusion along many directions and observing the direction of fastest diffusion, which corresponds to the longitudinal axis of the tract, we can determine the neural direction. At our institution we acquire diffusion weighted (DW) images of the LSP in the axial plane with *b*-values=0 and 900 $s\,mm^{-2}$ and 30 gradient directions. Fractional anisotropy (FA) and apparent diffusion coefficient (ADC) map calculation are performed in-line by the MRI scanner, and fibre tracts of the LSP can be calculated from several seed points placed at different levels close to the nerve roots. DTI with tractography does not replace anatomical plexus imaging provided with 2D T_1 and T_2 weighted sequences nor with the 3D STIR SPACE sequence. However, it may give additional information regarding the integrity of plexus fibres and their pattern of displacement or impairment with respect to the tumour mass, which is not always easy to diagnose with anatomical images alone [10]. The DTI, which was previously reserved for research purposes [11, 12], has recently started to claim its position in everyday clinical practice, and we believe that it plays an important role in surgical planning [6]. The primary potential application of DW neurography and DTI is in the assessment of tumoral pathology. We found that DW neurography with tractography reconstruction can reliably demonstrate the relationship between a tumour and its original nerve root, as well as fibre alterations, such as displacement, deformation or interruption.

Anatomy of the lumbosacral plexus

The lumbar plexus is formed by the anastomosis of the ventral rami of the first four lumbar nerves and in some cases of the last thoracic nerve. They form, respectively: the ilio-inguinal and iliohypogastric nerve (L1), the genitofemoral nerve (L1–L2), the femoral nerve (L2–L3–L4), the lateral cutaneous nerve of the thigh (L2–L3) and the obturator nerve (L2–L3–L4). (Figure 1a).

The femoral nerve is a mixed nerve and the largest terminal branch of the lumbar plexus. It provides motor innervation to the extensors of the knee, and sensory innervation to parts of the thigh, lower leg, foot and to the hip and knee joints.

The femoral nerve descends along the posterior part of the psoas muscle and then curves around and comes to rest on its antero-medial surface. It is situated in the iliac fascia between the two heads of the ilio-psoas muscle. It passes beneath the inguinal ligament lateral to the femoral vessels and the ilio-pectineal line, and exits from the external inguinal ring.

The sacral plexus is formed from the lumbosacral trunk and the ventral rami of the first three sacral nerves. The lumbosacral trunk comprises the whole of the ventral ramus of the fifth and a part of that of the fourth lumbar nerve; it appears at the medial margin of the psoas muscle and runs downward over the pelvic brim to join the first sacral nerve.

The nerves forming the sacral plexus unite to form the sciatic nerve (Figure 1), the terminal branch of the lumbosacral plexus (L4–S3). This is the longest and thickest nerve of the human body [13]. It is found in close proximity to the piriformis muscle, and exits the pelvis through the sciatic foramen, running between the greater trochanter of the femur and the ischial tuberosity and along the posterior part of the thigh, where it is divided into two branches: the tibial nerve and the common peroneal nerve.

The sciatic nerve innervates the skin of the lateral and posterior region of the leg, the articular capsule of the hip

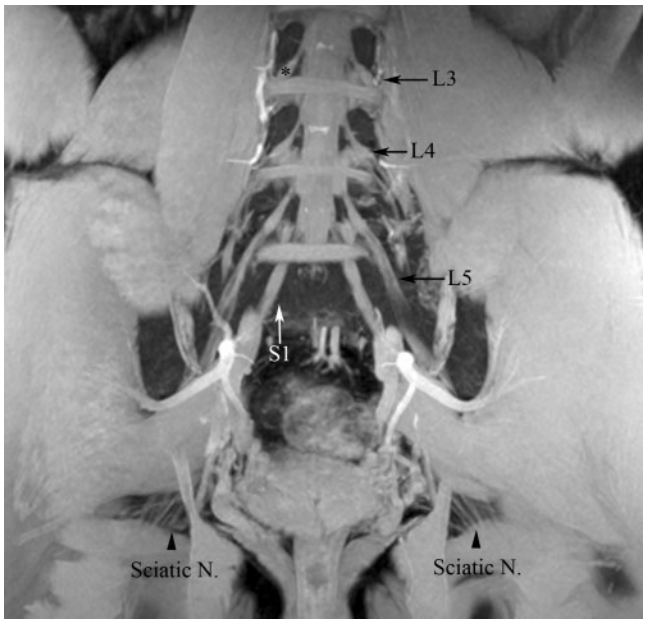

(a)

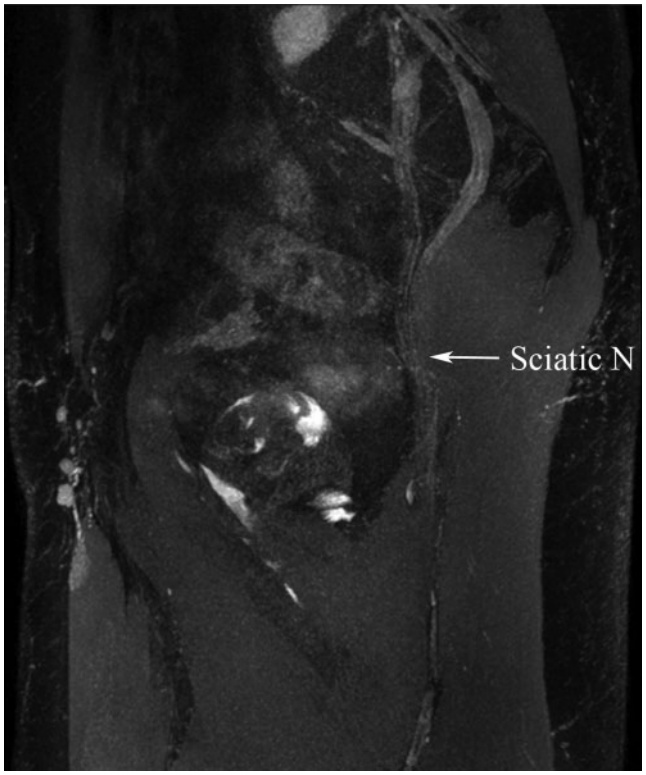

(b)

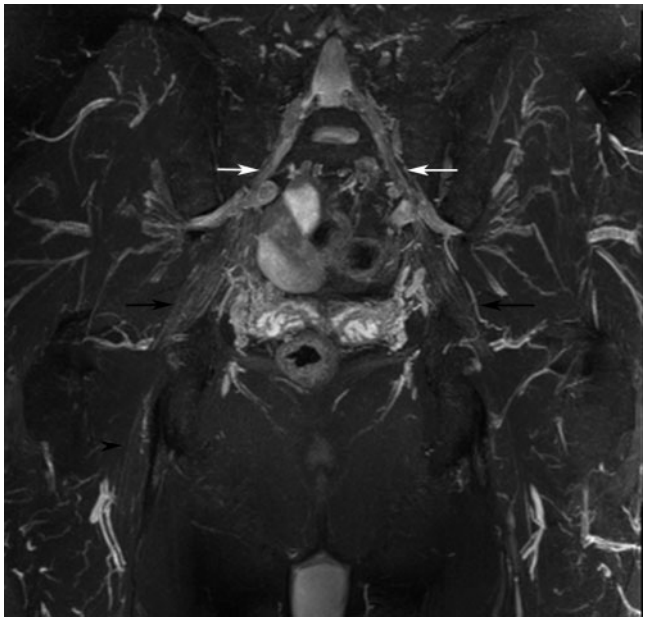

(c)

Figure 1. (a) Three-dimensional (3D) gradient echo T_1 weighted image (echo time: 4.6 ms, repetition time: 8.6 ms) demonstrating the normal anatomy of the lumbosacral plexus (LSP). Note the L3–S1 nerves forming the LSP (arrows), the spinal ganglion (asterisk) and the sciatic nerves (arrowheads). (b) A curved reformatted 3D short tau inversion-recovery sampling perfection with application-optimised contrasts using different flip angle evolutions image (echo time: 3.1 ms, repetition time: 8.4 ms) demonstrates the sciatic nerve (arrow). (c) A coronal reformatted 3D short tau inversion-recovery multiplanar image (echo time: 123 ms, repetition time: 1800 ms) demonstrates the origin of the sciatic nerve (white arrows) and its flat configuration (black arrow), which more distally becomes tubular (arrowhead).

joint, the muscles of the posterior part of the thigh and all the muscles of the leg and foot [14].

The collateral branches of the sacral plexus comprise the nerve to the obturator internus and superior gemellus muscles, the nerve to the quadratus femoris and inferior gemellus muscles, the nerve to the piriformis muscle, the superior and inferior gluteal nerves and the posterior cutaneous nerve of the thigh. The pudendal

nerve derives its fibres from the ventral rami of S2, S3 and S4. It passes between the piriformis and coccygeus muscles, and leaves the pelvis through the lower part of the greater sciatic foramen, crosses the spine of the ischium and re-enters the pelvis through the lesser sciatic foramen.

The pudendal nerve gives off the inferior rectal nerves. It soon divides into two terminal branches: the perineal nerve and the dorsal nerve of the penis or clitoris.

Pathologies

The origin of LSP pathologies can be neurogenic or related to the neighbouring tissues. Among the different types of lesions affecting the LSP we present:

(1) neoplastic pathologies
  (a) intrinsic plexus tumours (neurogenic tumours)
  (b) extrinsic tumours (non-neurogenic tumours)
(2) traumatic pathologies
(3) infectious pathologies
(4) gynaecological pathologies
(5) miscellaneous.

Neoplastic pathologies

Tumours can be classified as intrinsic or extrinsic depending on whether they are of neurogenic or non-neurogenic origin. Intrinsic tumours, which are the most common, can be benign (*i.e.* neurofibromas, schwannomas, perineurinomas) or malignant peripheral nerve sheath tumours (MPNST).

Extrinsic tumours are principally malignant (metastatic), whereas lipoma, myositis ossificans, lymphangioma, hemangioma and fibromatosis are the most common extrinsic benign lesions.

Intrinsic plexus neoplasms

Neurofibromas may be single or multiple and correspond to World Health Organization (WHO) grade 1. Lesions designated grade 1 generally include tumours with low proliferative potential and the possibility of cure following surgical resection alone [15]. They are encapsulated and not easily separated from the nerve. A neurological deficit is usually present following surgical treatment. They consist of mixed cells, including Schwann cells, ''perineural-like cells'' and fibroblasts [15–17]. They are most frequently subcutaneous rather than at the level of a peripheral nerve.

On MRI, neurofibromas appear as rounded or fusiform lesions that are hyperintense on T_2 and STIR imaging, are isointense to muscle on T_1 weighted sequences and are typically associated with marked post-contrast enhancement (Figure 2). Their differentiation from schwannomas remains difficult. Solitary neurofibromas are three times more common in women. Multiple neurofibromas may be associated with neurofibromatosis Type 1 (NF1) and they show no sex predilection. Sciatica is rarely a symptom of neurofibromas [18].

Plexiform neurofibroma is a subtype of neurofibroma exclusively observed in patients with NF1. It diffusely infiltrates the nerve structures and is principally located in the brachial and the sacral plexuses [18] (Figure 3).

Also called neurinomas or neurilemomas (Figure 4), *schwannomas* are slowly developing benign tumours that are well circumscribed, encapsulated, round or fusiform. They are derived completely from Schwann cells that originate from the neural sheath. They correspond to WHO grade 1 [15]. They measure from a few millimetres up to 10 cm in diameter and are eccentrically located in relation to the nerve. Schwannomas represent 8% of neural intracranial tumours, 85% of ponto-cerebellar angle tumours and 29% of neural root tumours. In approximately 90% of cases they are solitary and sporadic, whereas in 4% they are associated with neurofibromatosis Type 2 (NF2) [15]. Therefore, when multiple schwannomas are present, NF2 should be excluded. The treatment of these lesions is surgical when they become symptomatic. Relapse is rare and should raise suspicion of malignant transformation. They can present at any age, but are rare in children, with a peak incidence between 40–60 years of age. There is no sex predilection. The majority of these tumours are found outside the central nervous system. Generally they are asymptomatic or can be revealed by radicular compression.

On MRI, schwannomas are depicted as well-delineated, occasionally cystic lesions that appear hyperintense or heterogeneous on STIR and T_2 weighted images, isointense compared with muscle on T_1 weighted images and are associated with intense post-contrast enhancement (Figure 5). If the tumour is

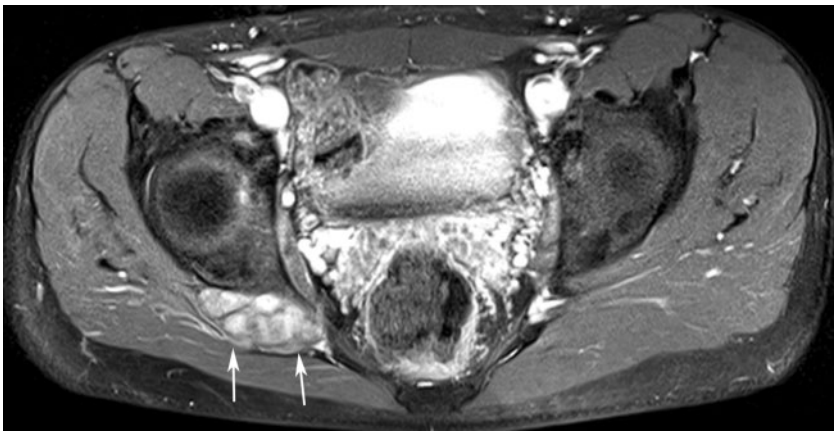

Figure 2. Contrast-enhanced T_1 fat-saturated axial image (echo time: 15 ms, repetition time: 667 ms) showing a very well-delineated and enhanced ovoid mass corresponding to a neurofibroma (arrows) situated at the right sciatic nerve in a patient with neurofibromatosis Type 1.

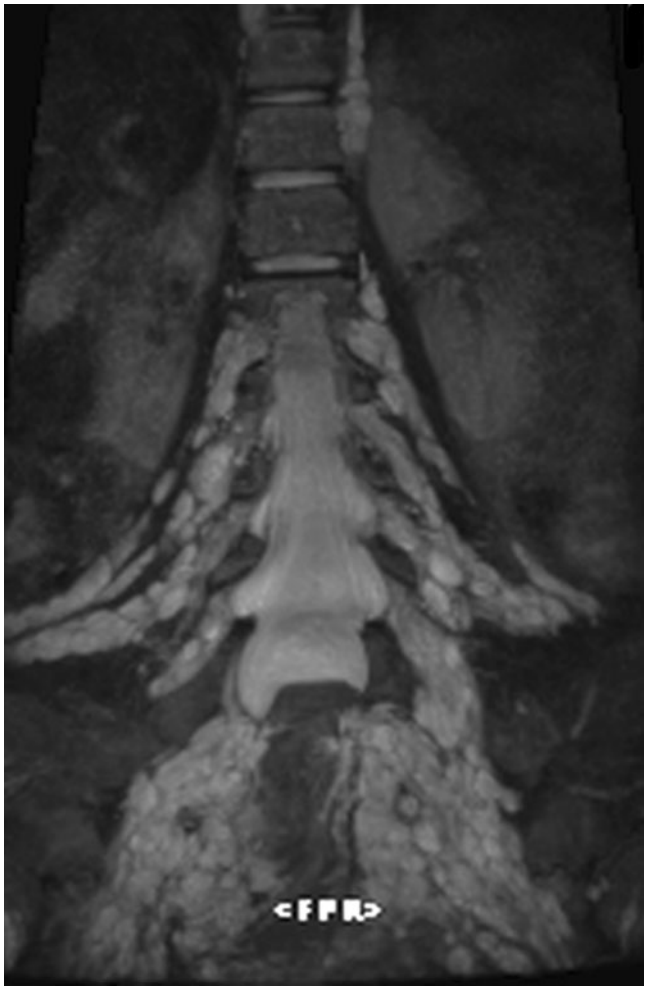

Figure 3. Three-dimensional short tau inversion-recovery multiplanar (echo time: 150 ms, repetition time: 2000 ms) reformatted coronal image showing plexiform neurofibroma of both lumbosacral plexuses.

situated in contact with a bony structure, bone scalloping might be present, which can be better demonstrated by CT imaging.

Perineurinoma is a rare benign tumour corresponding to 5% of neural tumours, originating from perineural cells and more specifically from the concentric cellular layer proliferation in the endonerve, responsible for its characteristic ''onion bulb'' appearance. This feature differentiates it from soft tissue perineuroma. It corresponds to WHO grade 1 [15]. Perineurinomas were formerly known by the term hypertrophic neuropathy, which is now actually recognised as a different tumoral entity. Perineuromas do not have a sex predilection and are found in children and young adults. The peripheral nerves of the extremities are principally affected, whereas cranial nerves are generally preserved. On imaging, perineuromas cause a regular tubular enlargement of the nerve and are hyperintense on STIR and T_2 weighted sequences, and hypointense on T_1 weighted sequences, with homogeneous enhancement after intravenous contrast administration. DTI is useful to show the exact limits of the lesion [16]. Treatment of these lesions is by complete surgical resection, following which they do not tend to recur.

MPNST are rare, arising either from pre-existing plexiform neurofibromas or as a spontaneous mutation. MPNST can look identical to their benign counterparts, but pain, progressive enlargement, irregular infiltrative borders, internal inhomogeneity and adjacent oedema are suggestive of malignant degeneration [19].

Extrinsic plexus tumours

Extrinsic plexus lesions are classified as malignant (metastasis) and benign (lipoma, myositis ossificans, lymphangioma, hemangioma and fibromatosis).

The LSP may be infiltrated or compressed by an extrinsic neoplasm emanating from the neighbouring tissues. Most commonly, the LSP is affected by non-neurogenic malignant intrapelvic tumours. Rectal cancer, gynaecological and prostatic malignancies, urinary bladder carcinoma, retroperitoneal sarcoma and lymphoma can cause plexopathy by direct spread or compression (Figure 6). Pelvic bone metastases, soft tissue metastases (*e.g.* to psoas muscle) and lymph node metastases may also be encountered and account for only 25% of sciatica related to extrinsic plexus tumours [20].

CT imaging of the abdomen and pelvis can be particularly helpful in revealing retroperitoneal or intrapelvic tumours, as well as bone metastases, responsible for extraspinal lumbosacral radiculopathy. However, in many cases the lesion can be missed on the initial lumbar CT scan because the scan area is too small to visualise the paraspinal soft tissues [21]. On MRI, the associated radicular lesions are hyperintense on T_2 and STIR sequences, and hypointense on T_1 weighted images associated with a significant post-contrast enhancement. Fat saturation sequences are essential, particularly at the level of the pelvis.

Traumatic pathologies

Most commonly, post-traumatic lumbosacral plexopathies occur in conjunction with severe bone fractures, especially of the pelvic girdle, the acetabulum and the sacroiliac joint. Pelvic region fractures may lead to avulsions or pre-ganglionic nerve lesions that are readily demonstrated on high resolution 3D T_2 weighted sequences [22] such as 3D CISS (constructive interference in steady state), 3D TrueFISP (fast imaging with steady state precession), FIESTA (fast imaging employing steady state acquisition) and DRIVE (driven equilibrium) sequences, particularly in the acute phase. In chronic cases their recognition is more challenging, particularly in the context of an unclear clinical history.

Sciatic nerve injury may also occur following proximal hamstring injuries/avulsions, especially in athletes. Oedema, inflammation and haematoma formed around the affected tendon may potentially compress the adjacent sciatic nerve.

Traction injuries to the LSP may be provoked by fracture or posterior hip dislocation (Figure 7) or during its reduction.

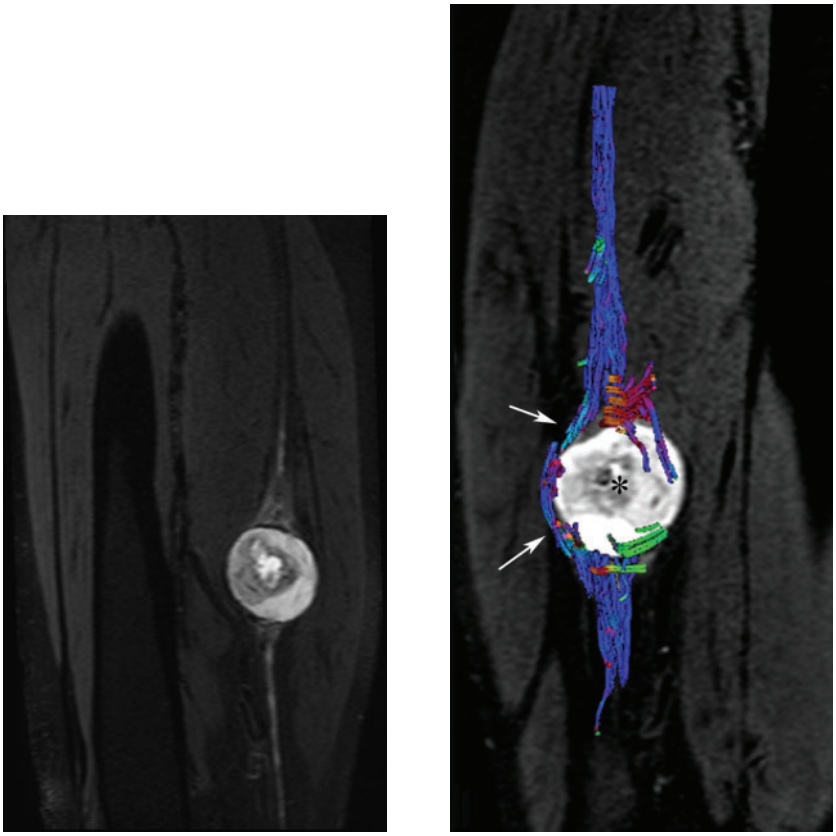

(a) (b)

Figure 4. (a) Three-dimensional short tau inversion-recovery multiplanar reformatted sagittal image (echo time: 60 ms, repetition time: 6558 ms) and (b) tractography (echo time: 77 ms, repetition time: 9200 ms) revealing a schwannoma arising from the sciatic nerve (a) with neural tract displacement [arrows in (b)], but no infiltration by the neurogenic mass [asterisk in (b)].

Figure 5. Contrast-enhanced T_1 fat-saturated coronal image (echo time: 10 ms, repetition time: 657 ms) demonstrating a cystic schwannoma originating from the right L3 nerve root (arrows).

Infectious pathologies

Iliopsoas, pelvic abscesses and gluteal abscesses are the principle causes of sciatic nerve infection and sciatica. Spondylodiscitis, infectious sacroiliitis (Figure 8), gastrointestinal pathologies such as diverticulitis and Crohn's disease, post-surgical complications and genitourinary infections account for the most common causes of an iliopsoas abscess. Iliopsoas muscle infection secondary to haematogenous dissemination occurs more rarely. Gluteal abscesses are occasionally encountered owing to infected haematomas and intramuscular injections. Sigmoid diverticulitis and tubo-ovarian infections are the main causes of pelvic abscesses.

Abscesses are seen as hyperintense collections on T_2 and STIR images with associated peripheral oedema, showing rim enhancement on T_1 contrast-enhanced images. In many of these cases (*e.g.* sigmoid diverticulitis), a lesion affecting the LSP can be suspected on the basis of a CT scan. If related symptoms of sciatica are present, MRI can confirm the diagnosis.

Gynaecological pathologies

Gynaecological conditions such as ectopic endometriosis, ovarian cysts and pregnancy may result in sciatica, with a tendency to affect the right side [23]. During the late stages of pregnancy or during delivery, compression of the LSP can occur between the foetal head and the pelvic

(a)

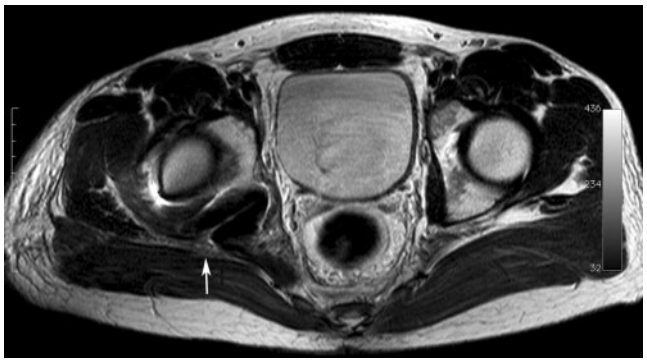

(b)

Figure 6. (a) Unenhanced sagittally reconstructed CT image showing a posterior fracture dislocation of the hip joint. (b) T_2 axial image after reduction shows the hyperintense and enlarged right sciatic nerve after hip reduction (arrow).

rim. Ectopic sciatic endometriosis should be suspected in women of reproductive age with periodic exacerbations of sciatica, known as cyclic sciatica. On MRI, extrapelvic sciatic endometriosis can be visible as endometrial foci in the vicinity of the nerve resulting in axonal nerve injury and Wallerian degeneration [24].

(a)

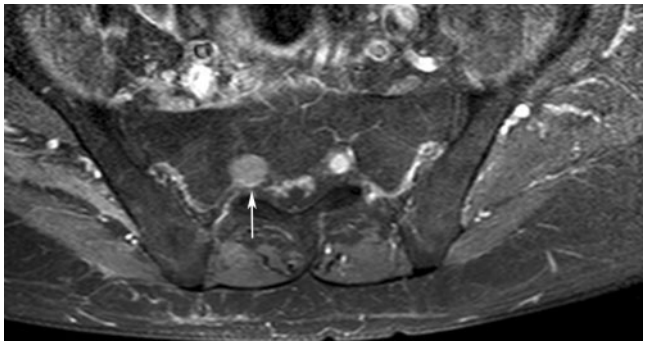

(b)

Figure 7. (a) Unenhanced T_1 coronal image (echo time: 12 ms, repetition time: 400 ms) and (b) enhanced fat-saturated axial T_1 image (echo time: 12 ms, repetition time: 400 ms), showing metastatic lesions in both ischial tuberosities [asterisks in (a)], atrophy of the glutei and proximal right thigh muscles [arrowheads in (a)] and secondary tumoral infiltration of the enlarged right sciatic nerve [arrows in (a, b)].

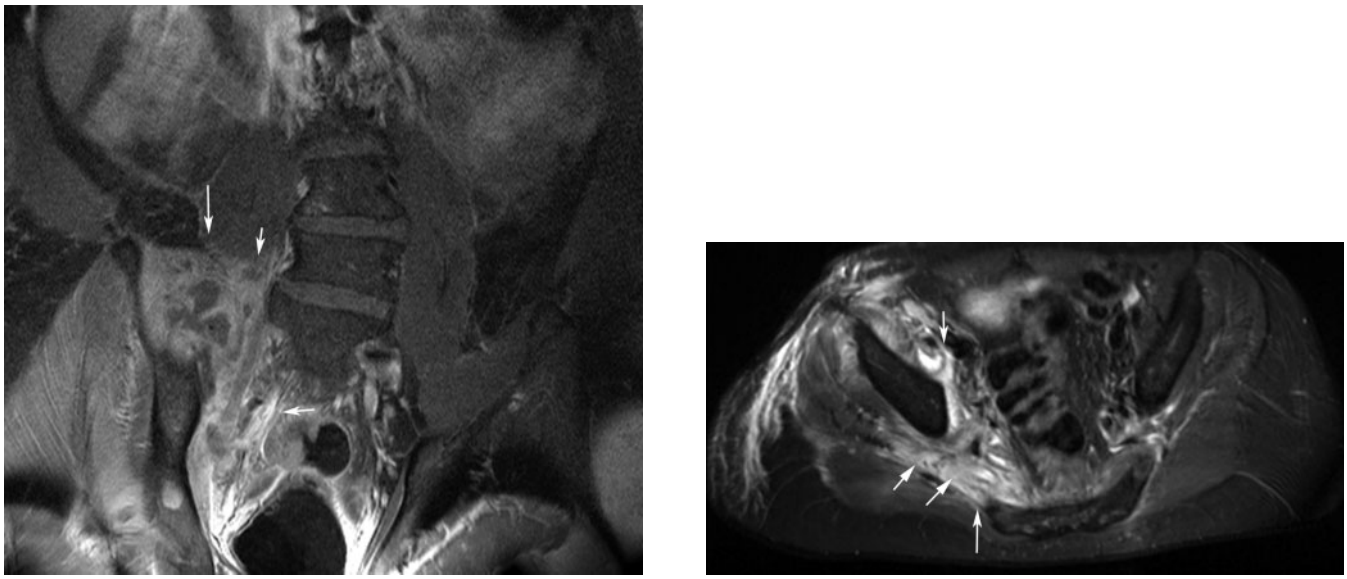

(a) (b)

Figure 8. Contrast-enhanced T_1 fat-saturated (a) coronal (echo time: 12 ms, repetition time: 400 ms) and (b) axial images illustrating a large abscess in the right psoas and glutei muscles in contact with the sciatic nerve (arrows).

Miscellaneous

The piriformis muscle can cause proximal irritation or compression of the sciatic nerve, referred to as ''piriformis syndrome''. Aetiologies of piriformis syndrome include muscular hypertrophy, myositis ossificans, muscular fibrosis, haematoma secondary to traumatic injury, sciatic nerve anatomical abnormalities or vigorous physical activity. Patients with piriformis syndrome will experience deep buttock pain with prolonged sitting and with internal hip rotation and adduction. Piriformis syndrome is a clinical diagnosis; MRI can demonstrate muscle asymmetry or signal intensity changes [17] and is mainly reserved to rule out other disorders associated with sciatica. Rarely, physical examination may reveal a tender palpable band of tissue corresponding to the piriformis muscle [25].

Piriformis syndrome and gynaecological conditions account for most cases of extralumbar sciatica [4, 23, 24, 26].

Pelvic cancer radiotherapy as a treatment for lymphoma, gynaecological and urological cancers may also induce lumbosacral plexopathy and sciatica due to fibrosis. However, unlike neoplastic lumbosacral radiculopathy, which is principally associated with severe pain, radiation plexopathy is accompanied mainly by limb weakness and swelling. Significant pain can occur in fewer than 25% of cases [27].

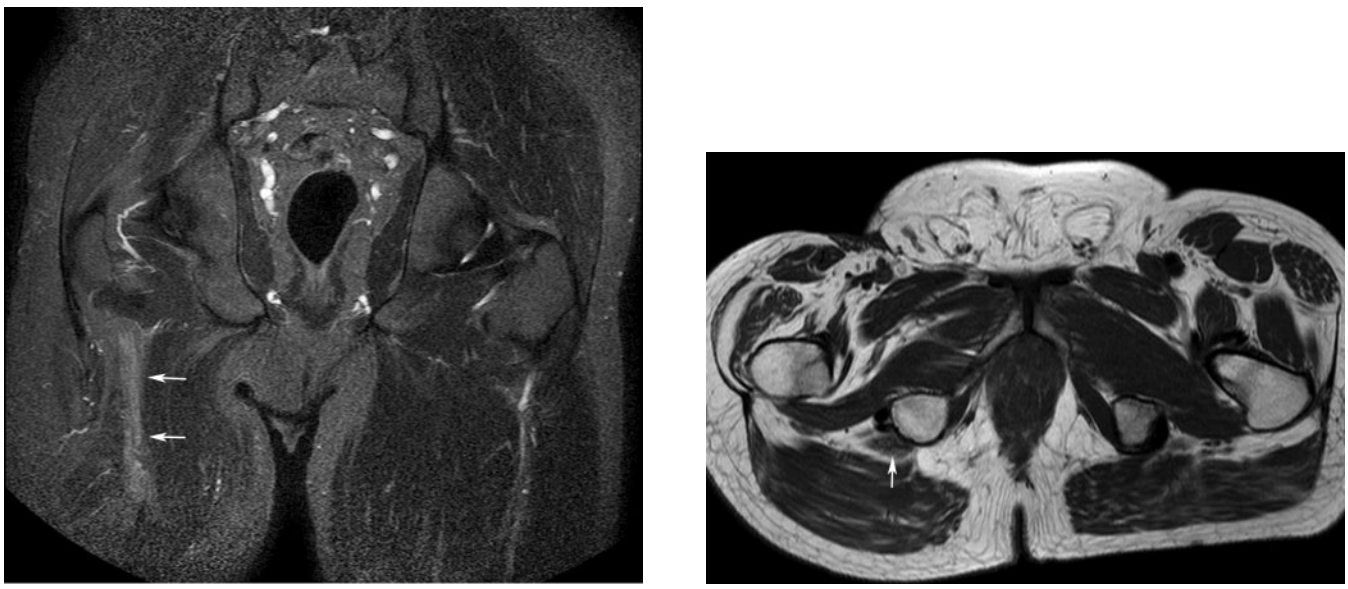

(a) (b)

Figure 9. (a) Short tau inversion-recovery coronal image (echo time: 60 ms, repetition time: 3685 ms) and (b) T_2 spin echo axial image (echo time: 16 ms, repetition time: 943 ms) showing enlarged and hyperintense right sciatic nerve after amputation (arrows).

Although extremely rare, osteochondroma (solitary or multiple) can affect the lumbar spine and the femoral neck, resulting in nerve root and sciatic nerve compression, respectively [28–30]. These lesions are well demonstrated on CT, but MRI is particularly useful for the depiction of the overlying cartilaginous cap, as well as the associated nerve compression.

Owing to the close anatomical proximity of the sciatic nerve to the gluteal and iliac vessels, varicose gluteal veins, congenital pelvic arteriovenous malformations and aneurysms of the distal aorta, the iliac and intrapelvic arteries, have been implicated in triggering sciatica through external compression [27, 31, 32]. Their decompression results in complete resolution of sciatica. Cases with varicosity-caused sciatica are limited in the literature review.

Iatrogenic sciatic nerve injuries have been reported and are usually caused by an injection in the buttock region, after total hip arthroplasty, hysterectomy or vascular surgery.

Rarely, paradoxical sciatic nerve stump hypertrophy can develop in young patients who underwent limb amputation, in contrast to neural atrophy, which is characteristic in older patients [33, 34] (Figure 9). Residual limb pain post amputation is often referred to as ''stump pain'' and has been described in up to 60% of patients [35]. Neuropathic stump pain can be successfully relieved by a peripheral nerve block [36, 37].

Conclusion

Although sciatica is most commonly caused by a herniated disc, knowledge of and familiarity with its extraspinal causes is important for an optimal therapeutic approach, considering its prevalence and the resulting personal, social and economic consequences. Imaging of the LSP is improving in accordance with evolution of MRI techniques. We believe that a combination of clinical findings and MRI utilising ''state of the art'' imaging protocols enables an accurate diagnosis of the cause of sciatica, and thus can guide appropriate treatment.

References

1. Yoshimoto M, Kawaguchi S, Takebayashi T, Isogai S, Kurata Y, Nonaka S, et al. Diagnostic features of sciatica without lumbar nerve root compression. J Spinal Disord Tech 2008;22:328–33.
2. Rohkmann R. Atlas de Poche de neurologie. Paris, France: Flammarion; 2003.
3. Vargas MI, Beaulieu J, Magistris MR, Della Santa D, Delavelle J. Clinical findings, electroneuromyography and MRI in trauma of the brachial plexus. J Neuroradiol 2007;34:236–42.
4. Chappell KE, Robson MD, Stonebridge-Foster A, Glover A, Allsop JM, Williams AD, et al. Magic angle effects in MR neurography. AJNR Am J Neuroradiol 2004;25:431–40.
5. Viallon M, Vargas MI, Jlassi H, Lövblad KO, Delavelle J. High-resolution and functional magnetic resonance imaging of the brachial plexus using an isotropic 3D *T*2 STIR (short term inversion recovery) SPACE sequence and diffusion tensor imaging. Eur Radiol 2008;18:1018–23.
6. Vargas MI, Viallon M, Nguyen D, Delavelle J, Becker M. Diffusion tensor imaging (DTI) and tractography of the brachial plexus: feasibility and initial experience in neoplastic conditions. Neuroradiology 2010;52:237–45.
7. Khalil C, Hancart C, Le Thuc V, Chantelot C, Chechin D, Cotten A. Diffusion tensor imaging and tractography of the median nerve in carpal tunnel syndrome: preliminary results. Eur Radiol 2008;18:2283–91.
8. Andreisek G, White LM, Kassner A, Tomlinson G, Sussman MS. Diffusion tensor imaging and fiber tractography of the median nerve at 1.5T: optimization of b value. Skeletal Radiol 2009;38:51–9.
9. Khalil C, Budzik JF, Kermarrec E, Balbi V, Le Thuc V, Cotten A. Tractography of peripheral nerves and skeletal muscles. Eur J Radiol 2010;7:391–7.
10. Tsuchiya K, Imai M, Tateishi H, Nitatori T, Fujikawa A, Takemoto S. Neurography of the spinal nerve roots by diffusion tensor scanning applying motion-probing gradients in six directions. Magn Reson Med Sci 2007;6:1–5.
11. Le Bihan D, Mangin JF, Poupon C, Clark CA, Pappata S, Molko N, et al. Diffusion tensor imaging: concepts and applications. J Magn Reson Imaging 2001;13:534–46.
12. Takagi T, Nakamura M, Yamada M, Hikishima K, Momoshima S, Fujiyoshi K, et al. Visualization of peripheral nerve degeneration and regeneration: monitoring with diffusion tensor tractography. Neuroimage 2009;44: 884–92.
13. Dietemann JL, Sick H, Wolfram-Gabel R, Cruz da Silva R, Koritke JG, Wackenheim A. Anatomy and computed tomography of the normal lumbosacral plexus. Neuroradiology 1987;1987:58–68.
14. Harnsberger HR, Osborn A, MacDonald A, Ross JS. Diagnostic and surgical imaging anatomy. Salt Lake City, UT: Amirsys; 2006.
15. Louis DN, Ohgaki H, Wiestler OD, Cavenee WK. WHO classification of tumours of the central nervous system. 3rd edn. Lyon, France: International Agency for Research on Cancer; 2007.
16. Merlini L, Viallon M, De Coulon G, Lobrinus JA, Vargas MI. MRI neurography and diffusion tensor imaging of a sciatic perineuroma in a child. Pediatr Radiol 2008;38:1009–12.
17. Stoller DW, Tirman FJP, Bredella AM. Diagnostic imaging: orthopaedics. 1st edn. Salt Lake City, UT: Amirsys; 2004.
18. Savva E, Vargas MI, Beaulieu JY, Truffert A, Burkhardt K, Lobrinus JA, et al. Giant plexiform neurofibroma in neurofibromatosis type 1. Arch Neurol 2010;67:356–7.
19. Stubblefield MD, O'Dell M. Cancer rehabilitation: principles and practice. New York, NY: Demos Medical Publishing; 2009.
20. Berger AM, Shuster JL, Von Roenn JH Jr. Principles and practice of palliative care and supportive oncology. 3rd edn. Philadelphia, PA: Lippincott, Williams & Wilkins; 2006.
21. Kleiner JB, Donaldson WF 3rd, Curd JG, Thorne RP. Extraspinal causes of lumbosacral radiculopathy. J Bone Joint Surg Am 1991;73:817–21.
22. Ramli N, Cooper A, Jaspan T. High resolution CISS imaging of the spine. Br J Radiol 2001;74:862–73.
23. Yoshimoto M, Kawaguchi S, Takebayashi T, Isogai S, Kurata Y, Nonaka S, et al. Diagnostic features of sciatica without lumbar nerve root compression. J Spinal Disord Tech. 2009;22:328–33.
24. Pham M, Sommer C, Wessig C, Monoranu CM, Pérez J, Stoll G, et al. Magnetic resonance neurography for the diagnosis of extrapelvic sciatic endometriosis. Fertil Steril 2010;94:351.e11–14.
25. Thomas Byrd JW. Piriformis Syndrome. Oper Tech Sports Med 2005;71–9.
26. Güvençer M, Akyer P, Iyem C, Tetik S, Naderi S. Anatomic considerations and the relationship between the piriformis muscle and the sciatic nerve. Surg Radiol Anat 2008;30: 467–74.

27. Ballantyne JC, Fishman SM, Rathmell JP. Bonica's management of pain. 4th edn. Philadelphia, PA: Lippincott, Williams & Wilkins; 2009.
28. Turan Ilica A, Yasar E, Tuba Sanal H, Duran C, Guvenc I. Sciatic nerve compression due to femoral neck osteochondroma: MDCT and MR findings. Clin Rheumatol2008;27:403–4.
29. Fiumara E, Scarabino T, Guglielmi G, Bisceglia M, D'Angelo V. Osteochondroma of the L-5 vertebra: a rare cause of sciatic pain: case report. J Neurosurg 1999;91(Suppl. 2):219–22.
30. Paik NJ, Han TR, Lim SJ. Multiple peripheral nerve compressions related to malignantly transformed hereditary multiple exostoses. Muscle Nerve 2000;23:1290–4.
31. Maniker A, Thurmond J, Padberg FT Jr, Blacksin M, Vingan R. Traumatic venous varix causing sciatic neuropathy: case report. Neurosurgery 2004;55:1224.
32. Bendszus M, Rieckmann P, Perez J, Koltzenburg M, Reiners K, Solymosi L. Painful vascular compression syndrome of the sciatic nerve caused by gluteal varicosities. Neurology 2003;61:985–7.
33. Hill SC, Baker AR, Barton NW, Wexler LH, Scott LJ. Sciatic nerve: paradoxic hypertrophy after amputation in young patients. Radiology 1997;205:559–62.
34. Kerimoglu U, Canyigit M. Paradoxic hypertrophy of the sciatic nerve in adult patients after above-knee amputation. Acta Radiol 2007;48:1028–31.
35. Dobrogowski J, Przeklasa-Muszynska A, Wordliczek J. Persistent post-operative pain. [In Polish.] Folia Med Cracov 2008;49:27–37.
36. Fischler AH, Gross JB. Ultrasound-guided sciatic neuroma block for treatment of intractable stump pain. J Clin Anesth 2007;19:626–8.
37. Van Geffen GJ, Bruhn J, Gielen MJ, Scheffer GJ. Pain relief in amputee patients by ultrasound-guided nerve blocks. Eur J Anaesthesiol 2008;25:424–5.